



RESEARCH LETTER

10.1002/2015GL066852

Key Points:

- Hybrid-analogue rock deformation experiments at PT using basalt and PMMA
- AE monitoring the formation of tensile fractures and subsequent viscous fluid flow
- Fracturing and fluid movement are characterized by different frequency spectra

Supporting Information:

- Figure S1 and Movies S1–S3 Captions
- Movie S1
- Movie S2
- Movie S3
- Data Set S1

Correspondence to:

R. R. Bakker,
richard.bakker@erdw.ethz.ch

Citation:

Bakker, R. R., M. Fazio, P. M. Benson, K.-U. Hess, and D. B. Dingwell (2016), The propagation and seismicity of dyke injection, new experimental evidence, *Geophys. Res. Lett.*, *43*, 1876–1883, doi:10.1002/2015GL066852.

Received 2 NOV 2015

Accepted 23 JAN 2016

Accepted article online 28 JAN 2016

Published online 4 MAR 2016

The propagation and seismicity of dyke injection, new experimental evidence

Richard R. Bakker¹, Marco Fazio², Philip M. Benson², Kai-Uwe Hess³, and Donald B. Dingwell³

¹Geological Institute, ETH Zürich, Swiss Federal Institute of Technology, Zürich, Switzerland, ²Rock Mechanics Laboratory, School of Earth and Environmental Sciences, University of Portsmouth, Portsmouth, UK, ³Department of Earth and Environmental Sciences, Ludwig Maximilians Universität, Munich, Germany

Abstract To reach the surface, dykes must overcome the inherent tensile strength of the country rock. As they do, they generate swarms of seismic signals, frequently used for forecasting. In this study we pressurize and inject molten acrylic into an encapsulating host rocks of (1) Etna basalt and (2) Comiso limestone, at 30 MPa of confining pressure. Fracture was achieved at 12 MPa for Etna basalt and 7.2 MPa for Comiso limestone. The generation of radial fractures was accompanied by acoustic emissions (AE) at a dominant frequency of 600 kHz. During “magma” movement in the dykes, AE events of approximately 150 kHz dominant frequency were recorded. We interpret our data using AE location and dominant frequency analysis, concluding that the seismicity associated with magma transport in dykes peaks during initial dyke creation but remains significant as long as magma movement continues. These results have important implications for seismic monitoring of active volcanoes.

1. Introduction

Seismic signals are a key monitoring tool for assessing the unrest and eruptive state of active volcanoes [e.g., McNutt, 1996; Chouet, 2003]. A wide range of seismicity is observed, ranging from volcano tectonic events (e.g., fracturing of rocks) to low-frequency harmonic tremor thought to be driven by fluid migration within the fractured edifice [e.g., Chouet, 2003]. The analysis of such seismic data sets includes tools such as (1) 3-D location, (2) event rate acceleration in order to forecast an edifice [e.g., Kilburn, 2012] or magma failure time [Lavallée et al., 2008], and (3) the changing spectral characteristics of the normalized waveforms to better understand the relative proportion of fracturing versus fluid/magma movement [e.g., Burlini et al., 2007; Benson et al., 2008]. While all these methods have proven useful in situations that have resulted in eruption, such as the 1991 eruption of Mount Pinatubo [Mori et al., 1996] and the eruptive period between 2004 and 2008 at Mount St. Helens [Kendrick et al., 2012], a great many cases exist where increasing seismic event rates have not resulted in eruption. This is often attributed to magma, in the form of dykes, stalling at depth [De Natale et al., 1997]. This is supported by field observations of arrested dykes [e.g., Gudmundsson, 2003] and recent research that has focused on the mechanics of dyke arrest [e.g., Gudmundsson and Brenner, 2004; Gudmundsson, 2011] due to Cook-Gordon delamination, stress barriers, and elastic mismatches. However, these “false alarms” remain poorly understood. While there are plenty of examples where seismicity is correlated to movement of dykes through the country rock [e.g., Gudmundsson et al., 2014; Browning and Gudmundsson, 2015; Sigmondsson et al., 2015], it remains unclear how this movement results in the seismicity that is recorded at the surface.

To investigate some of these dyke intrusion and propagation processes, previous laboratory work has employed analogue materials such as dyed water or glycerin injected into a second medium [e.g., Taisne and Tait, 2011]. Such analogue studies have proven extremely useful but are so far restricted to room pressure/temperature and cannot record any seismicity generated at the moving dyke tip. In contrast, laboratory rock deformation studies of volcanic processes employing acoustic emission (AE) as proxy for tectonic earthquakes [e.g., Kilburn, 2012] have produced data that are qualitatively similar to many types of volcano seismic signals. However, these are largely restricted to deformation in the compressional regime. Moreover, the use of AE is restricted to modest temperatures due to the temperature limits of the sensors (~200°C, [Benson et al., 2010]). To date, the investigation of rock fracture in tension due to an overpressurized (dyke-like) conduit at in situ temperatures [Benson et al., 2012] has employed only two AE sensors, located remotely and connected to the “hot zone” via waveguides. We know that the use of multiple AE sensors is a potentially very powerful tool to examine such processes on a small scale, particularly in terms of spatiotemporal frequency

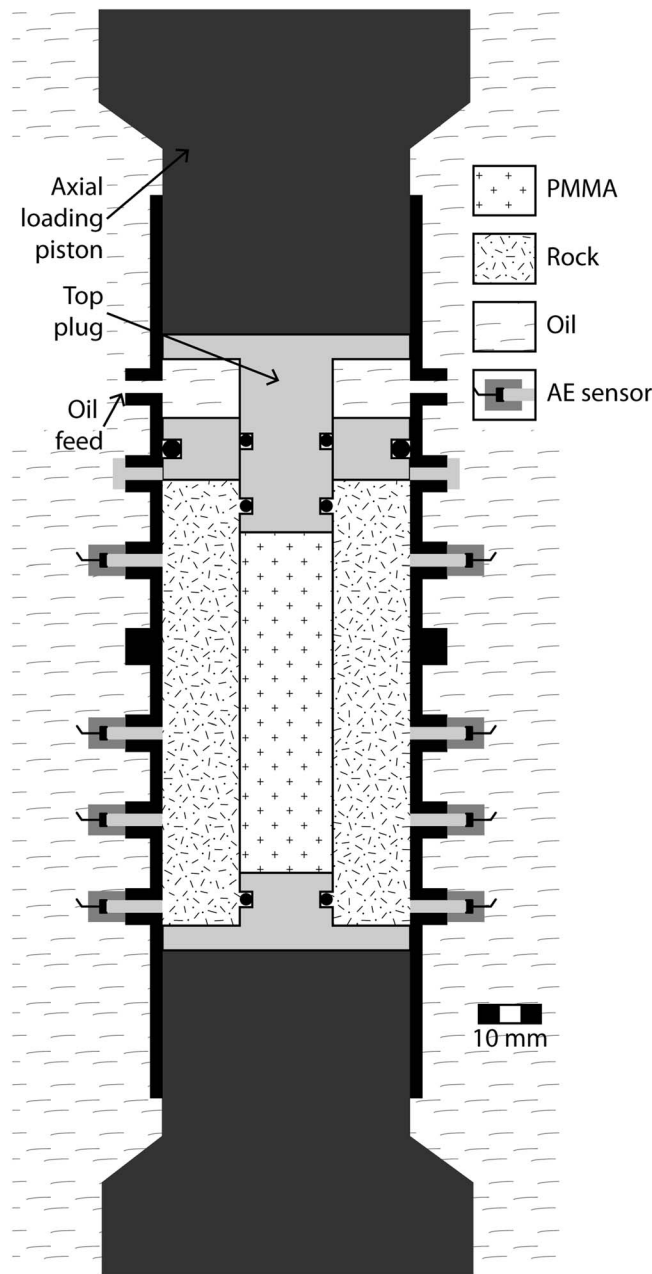


Figure 1. Simplified schematic (cross section) of the sample assembly which sits inside the triaxial pressure vessel. In this setup, the top piston (normally providing an axial principal stress, σ_1) is used to apply a stress to the top area of a molten PMMA plug that expands laterally, pressurizing the entire conduit and applying a tensile stress to the inner surface of the wall rock (Etna basalt or Comiso limestone in this work). The system is encapsulated by a rubber jacket embedded with 12 AE sensors for the detection of acoustic emission (AE), as well as a steel lower and floating, sealed, top annulus.

inner wall jacket. In our experiments the pressurizing medium is a rod of poly(methyl methacrylate) (PMMA or “Plexiglas”), a viscoelastic material that is molten at the temperature of the experiment (175°C). PMMA is ideal for our purpose as its glass transition temperature (T_g) occurs at a temperature of $\sim 100^\circ\text{C}$ (depending on composition) and behaves as a liquid when used at temperatures above T_g and appropriate time scales. Further, its Newtonian viscosity-temperature relationship is well known ($\sim 10^5$ Pa s at 175°C, see

analysis [e.g., Burlini *et al.*, 2007]. Therefore, in this study we investigate the process of dyking in volcanic edifices by using an optimized hybrid composed of elements of both of the above techniques. Below, we describe the initial results of a technique that operates at elevated temperatures using an analogue material but with an array of AE sensors so that the dyke initiation and movement may be analyzed.

It has been well established that dykes form in two stages: (1) the rapid initiation and opening of a mode 1 fracture, followed by (2) the infill of that fracture by a fluid. If the fluid is sufficiently pressurized, it exerts that pressure on the walls of the fracture, causing the fracture tip to propagate [e.g., Brenner and Gudmundsson, 2004]. Thus, dyking is a key magma transport process especially during the approach of magma to the surface. Both stages are likely to be seismogenic and that seismicity can be used to infer processes at depth in subvolcanic systems. Here we report the results of experiments including both stages, including the seismic characteristics of dyke injection process at elevated pressure and temperature conditions.

2. Methods

Our experiments employ a standard triaxial apparatus modified to incorporate an internal sample assembly (Figure 1) which has been designed to apply a tensile stress to the inner surface of a conduit or “borehole” as described by Benson *et al.* [2012]. This setup is similar to that of classic hydraulic fracturing studies [e.g., Hoskins, 1969; Santarelli and Brown, 1989; Vinciguerra *et al.*, 2004] with two important exceptions: (1) in the material types and (2) the lack of

Hieber and Chiang [1992]). The permeability of the host rock is sufficiently low that PMMA seepage through the host rock has an insignificant effect on the time scale of the experiment (Etna basalt [Fortin et al., 2011] and Comiso limestone [Bakker et al., 2015]). The use of PMMA at elevated temperatures has the benefit that the PMMA volume entering the fracture will solidify when the temperature falls below T_g , thereby preserving the geometry of the fracture for later characterization. Unlike earlier work [e.g., Benson et al., 2012], the new apparatus is able to apply a confining pressure (oil) to simulate modest burial depths, as well as using a 12 piezoelectric sensor array, made possible due to the lower temperatures imposed.

Our initial experiments employed samples of basalts obtained from lava flows on Mount Etna. We chose this rock type as it is considered a representative volcanic rock in a wide range of investigations, including seismic velocities [Vinciguerra et al., 2005], cyclic loading experiments in compression [Heap et al., 2009], and tension [Benson et al., 2012]. Recent work at elevated temperatures (R. R. Bakker, Understanding basement processes in sub-volcanic settings by laboratory measurements, PhD thesis, ETH Zürich, manuscript in preparation, 2016) has found that Etna basalt does not show a deviation in mechanical behavior until the temperature exceeds 700°C. Although these tests were performed in compression (at 50 MPa of confinement), we assume that this is also true in tension, allowing us to interpret the results over a wide range of temperature conditions.

Samples were coaxially drilled using a dual diamond drill bit so as to ensure a constant wall thickness. Samples were cut to 72 mm length, with an outer diameter of 40 mm and a 15 mm bore, resulting in a 12.5 mm wall thickness. The bore was filled with a 15 mm diameter PMMA rod, of approximately 55 mm length. The top and bottom parts of the inner hole were sealed using steel plugs, fitted with high-temperature resistant O rings. In order to impose a stress on the PMMA rod and thus pressurize the inner wall of the rock, the top plug is free to move into the sample bore through a central hole in the assembly. To allow movement, the space between the piston and rock sample is left open to the confining pressure. This provides a compensating pressure on the piston, as well as an axial stress on the sample (equal to the radial stress, see Figure 1). The entire setup is jacketed using an engineered nitrile jacket made from high-temperature rubber, which includes 12 ports for AE sensors.

The sample assembly is installed in a conventional triaxial compression apparatus capable of confining pressures of 100 MPa and fitted with an external furnace capable of reaching 200°C. Confining pressure and axial load are servo-controlled by two screw jack volumeters. AE are recorded on an array of 12 piezoelectric sensors, with signals preamplified by 60 dB prior to being split between two separate recording systems. The first system operates in “triggered” mode whereby discrete waveforms are recorded whenever any one of the 12 channels exceeds a predetermined voltage threshold. The second system records the waveform continuously to high-speed hard disk storage. Both systems digitize the signals at 10 MHz and at 16 bit resolution. Posttest, an automated picking routine (ITASCA-IMAGE “InSite” seismic processor), was used to obtain P wave arrivals for each sensor that were manually checked and corrected when necessary. In order to avoid refracted and reflected waves from the rock-PMMA interface, we chose to only locate the events using the sensors with the lowest arrival times, from the half of the array nearest to the generated fracture, as it is likely that these waves have only traveled directly through the rock from event location to sensor and are not refracted or reflected.

Using the above method and protocols, we have investigated two interrelated scenarios: (1) the increase of a conduit overpressure (compared to confinement pressure) with constant confinement pressure in which a new fracture (dyke) is generated and (2) the character of the continuous AE recorded once the fracture and dyke have formed. A confining pressure of 30 MPa was applied, simulating a depth of approximately 1.5 km, and a constant displacement rate for the top piston movement of 1 $\mu\text{m/s}$ was used. In both cases a basic AE location, using the radial statistics of event direction frequency as taken from the relevant aspect of the array (avoiding path/interface effects), is mapped and compared to the pressures required to open and sustain the fracture. After each test the samples were returned to a hydrostatic stress state before cooling down to room temperature.

3. Results

Figure 2 shows (1) the conduit overpressure and (2) the AE hit rate as a function of time for the Etna basalt (Figure 2a) at 175°C. The conduit pressure rises quickly in the first 150 s as initial pressurization of the molten PMMA occurs, after which the AE hit rate becomes measurable. After ~800 s a clear increase in AE hit rate coincides with a slowing conduit pressurization rate. Pressurization continues to a calculated peak

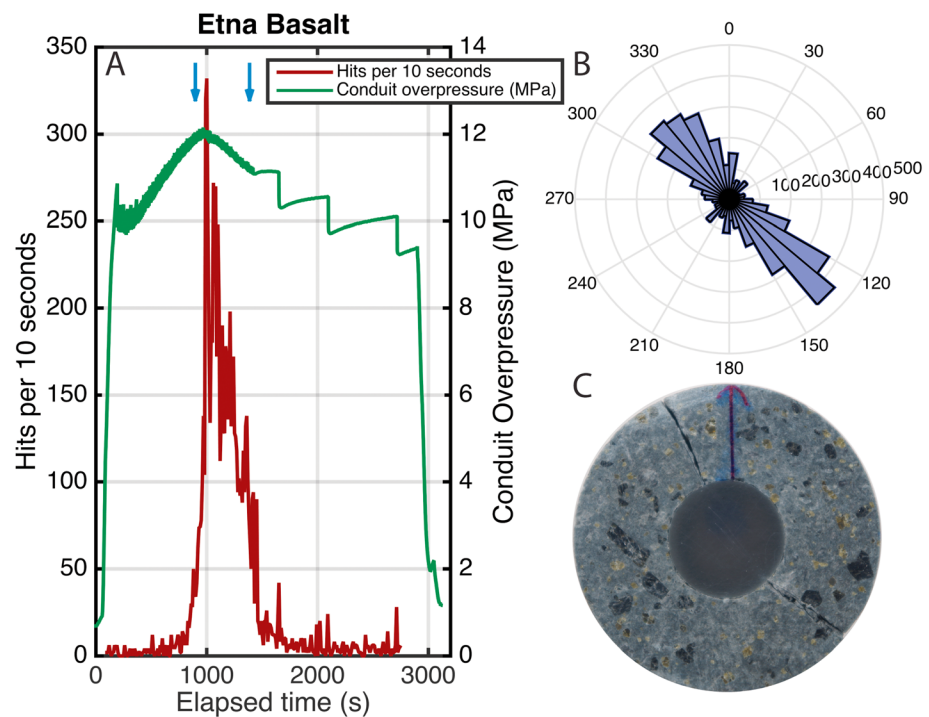


Figure 2. (a) Radial pressurization of Etna basalt at 175°C peaks at a conduit pressure of 12 MPa, coinciding with a peak in acoustic emission hit rate of approximately 335 hits per 10 s interval, after which point the conduit pressure falls, suggesting fracture of the wall rock. (b) AE location of the AE radial position suggests two dominant fracture positions, which is in agreement with (c) posttest examination of the sample.

overpressure of 12 MPa at which point a spike in AE is recorded and a fall in conduit pressure. This is likely to represent the initial fracture. Continued movement of the pressuring piston did not yield any further increase in conduit pressure, and AE hit rate falls at approximately 1400 s to prefracture levels, with minor peaks associated with stress drops in the order of 1 MPa. At 2750 s the conduit stressed was released (to hydrostatic conditions) and experiment was concluded. AE location data from the experiment (Figure 2b) indicated that two fractures formed at 180° with a well-clustered center. Importantly, these data agree well with posttest visual inspection (Figure 2c).

Our further experiments employed Comiso limestone (Figure 3) also at 175°C. They show a generally similar pattern. Conduit pressurization is initially slower, reaching a peak of approximately 7.2 MPa at 1000 s. The onset of AE occurs very rapidly, at 700 s, with a peak AE hit rate of only five hits per 10 s (compared to a maximum hit rate in the Etna basalt experiment of over 300 hits per 10 s). A clear break in slope in the conduit pressurization curve is seen at 800 s. However, continued pressurization likely results in failure at 1000 s at which time a second spike in AE hit rate is also recorded. After this time, the conduit pressure decreases, and AE activity rapidly subsides. At 2100 s the piston advance is stopped and the PMMA is allowed to relax, a process which is accompanied by minor AE. At 3000 s the conduit stressed is released and the experiment is terminated. Data from radial AE location (Figure 3b) are relatively poorly focused but nevertheless contain indications of radial fracture at 45°, 120°, 235°, and 300° (Figure 3c). These orientations generally match visual characterization of the fractures from postexperiment imaging in all but the 45° direction. In addition, considerably fewer AE hits were recorded (i.e., < 10 events per sector). Due to these limitations, and the fact that this unit is found deeper in the Etnean basement (likely at temperatures beyond the brittle to ductile transition, see Bakker *et al.* [2015]), we applied our main focus below to the basalt experiments, including the analysis of the generated AE and posttest samples.

Spectral analysis of the AE data is shown in Figure 4. The examples of waveform data shown (indicated by arrows in Figure 2a) were obtained during the main fracturing event and the PMMA movement, respectively. The waveform taken at 900 s (fracture) illustrates many of the classical features of an impulsive AE event with a rapid onset, short coda, and significant power across a broad frequency band to approximately 600 kHz

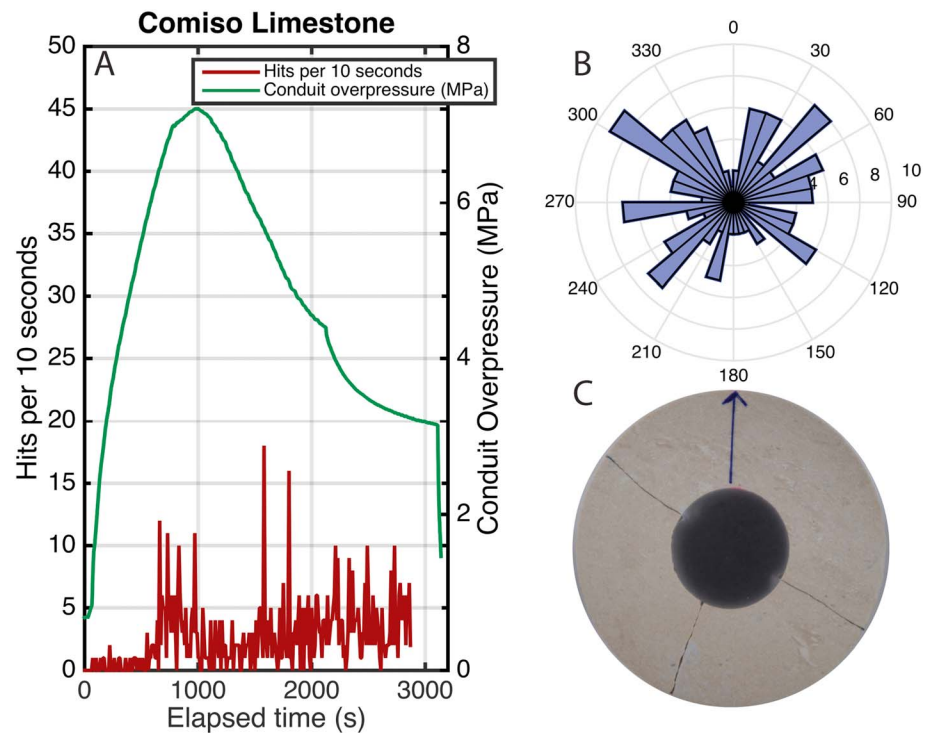


Figure 3. (a) Radial pressurization of Comiso limestone at 175°C peaks at a lower pressure of 7.2 MPa with a longer buildup. AE is lower than the equivalent data for the basalt, with two spikes in AE rate of approximately 11 and 18 hits per 10 s interval. The former of these AE peaks coincides with a break in conduit pressure increase followed by prominent decrease in pressure, interpreted as the failure of outer shell. (b) Radial AE location exhibits a wide range of fracture orientations, with three of these directions agreeing with (c) posttest inspection of the sample.

(Figure 4a). Conversely, the example of waveform data from the postfracture segment at 1400 s (Figure 4b) shows a very different character. Typical waveforms have a highly emergent nature, with a protracted coda exhibiting the type of ringing or resonance frequently seen during harmonic tremor seismic activity. The spectrogram analysis is consistent with this character (Figure 4b) illustrating a relatively monochromatic power spectrum centered at approximately 150 kHz and little power at frequencies over 250 kHz.

Posttest examination of the Etna samples illustrates the close match between fracture sets and AE data, with two fractures generated in the Etna sample. The PMMA has clearly intruded into the opened fracture, preserving the analogue dyke in situ after the sample has quenched, as designed. This is illustrated in a montage of X-ray computed tomography images (Figure S1 and Movies S1 to S3 also presented in the supporting information).

4. Discussion

Formation of an extensional fracture is the first stage in dyke propagation, requiring the pressurizing fluid (here magma) to overcome the tensile strength of the country rock in a mode 1 fracture and then to propagate as a feeder dyke [e.g., Gudmundsson, 2002]. Such features thus occur in both natural systems and hydrocarbon extraction technologies such as shale gas hydraulic fracturing [Rivalta *et al.*, 2015]. Despite their importance, the precise pressures required for this mechanism to operate are poorly known. This is especially true for magmatic systems. Here a viscoelastic analogue “magma” (PMMA) has been used to generate thin dyke-like structures in both a classically “brittle” material (represented by the basalt) and a slightly more ductile unit (represented by the Comiso limestone); both of which occur as rock types in subvolcanic basement and edifice. Both of these materials are well studied in the rock mechanics and rock physics literature [e.g., Heap *et al.*, 2009; Bakker *et al.*, 2015]. In the case of the basalt, a clear and obvious fracture set is propagated when internal pressure exceeds 12 MPa. This is in general agreement with previous work at magmatic temperatures [Benson *et al.*, 2012], where a conduit pressure of 15 MPa was required at a temperature of 918°C. A key

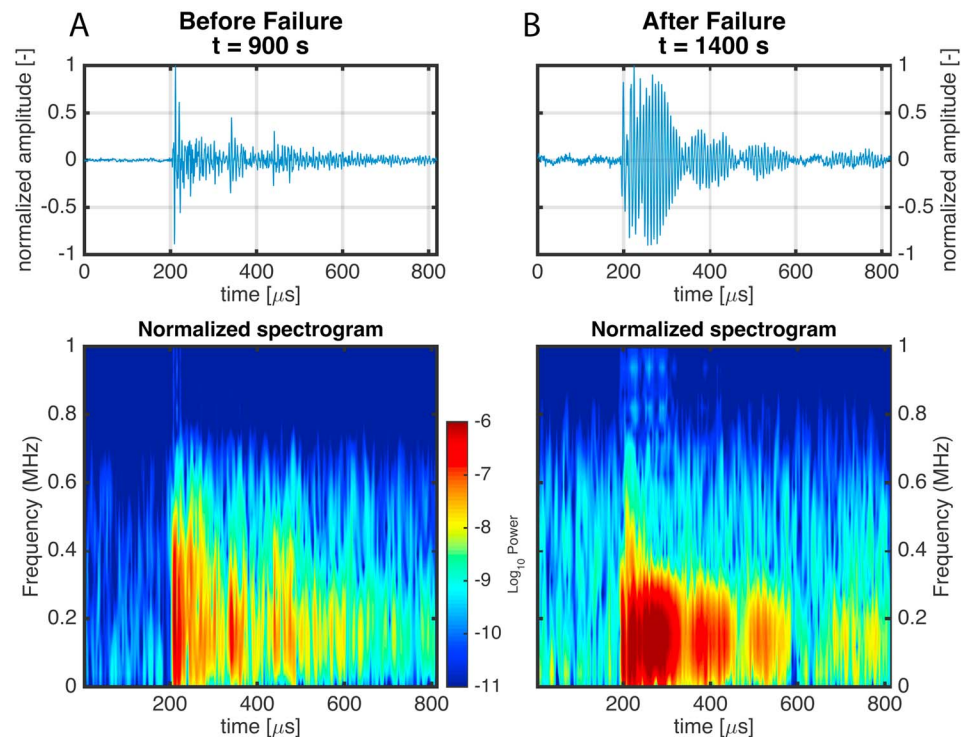


Figure 4. (a) Events during the initial fracture of the Etna basalt shell (arrow in Figure 2, approximately 900 s) show numerous features of the classical volcano tectonic waveform such as a sharp onset. (b) In contrast, waveforms collected after the pressure drop at approximately 1400 s, after fracture formation and during ingress of molten PMMA into the generated fracture, exhibits features of the so-called low-frequency (LF) type events such as a long coda and resonant or “ringing” nature. Spectrograms of the waveforms support this interpretation, showing polychromatic features characteristic of (c) volcano tectonic-type waveforms during fracture, where power is spread between 10 kHz (hardware filter minimum) and approximately 600 kHz. In contrast, (d) LF-type waveforms collected during PMMA ingress have monochromatic features with the majority of spectral power centered around 150 kHz.

advantage of the current experimental adaptation lies in the more advanced AE setup with which to chart the AE preferential directions (via a statistical approach) and to analyze the character of the recorded waveforms. It is this tool that reveals key differences between the emitted AE, and by extension field seismicity, during the different phases of dyke generation, which relies primarily on a mechanical generation, and the movement of the viscous magma through the fracture.

The magnitude and number of AE recorded are significantly greater in the basalt experiment. This likely results from the greater strength of the basalt with respect to the limestone, whereby fracturing is associated with larger stress releases than those responsible for the AE generated by fracturing of limestone. It is, indeed, a well-known observation that calcite-rich rocks produce fewer AE than most rocks with other mineral composition [e.g., *Cartwright-Taylor et al.*, 2014]. This behavior is reflected in both the statistics of the recorded AE and the location of those AE around the sample.

As demonstrated in previous work at much higher temperatures [*Benson et al.*, 2012], and in both cases, the recorded AE serves as a useful proxy for determining when the sample fails. This consistency of old and new results confirms the utility of the use of a lower temperature analogue at 175°C, with similar injected structures observed (Figure S1) and similar pressures required to promote the initial mode 1 failure.

A major area of current research in volcanic active areas is the occurrence of intense seismicity which is not followed immediately by eruption. Such “seismic crises” cause significant alarm to the local authorities and population and have occurred in densely populated areas such as the Campi Flegrei caldera around the city of Naples, Italy [*D’Auria et al.*, 2015]. Recent work has suggested that fluid migration plays a significant role in the local deformation (uplift) as well as the seismicity [e.g., *De Natale et al.*, 1997; *Battaglia et al.*, 2006], and the debate on the relative roles of hydrothermal and magmatic contributions to unrest events in this area

continues to this day. Here we observe that after the initial fracturing (analogous to dyke emplacement) not only the AE rate subsides (despite constant deformation/fluid injection rates) but also the conduit pressure continues to decrease. We link the reduction in AE in the experiments to the deflating caldera in nature and suggest that as magma stalls within newly established dykes at depth, a decrease in pressure occurs (assuming that inflow from deeper reservoirs is significantly slower than outflow through the dyke), as observed in our experiments. This is matched by a concomitant decrease in seismic event rates, also observed in our experiments, although it is noted that the rate does not fall off completely, unlike field seismic data as described in *Browning and Gudmundsson* [2015]. Finally, we note that the character of the AE changes significantly before and after fracturing (dyke) formation from the characteristic high frequency of brittle fracture to something resembling a resonance that is often taken as an indicator of fluid movement [e.g., *Chouet*, 1996], further supporting the idea that the established conduit is influencing the character of seismicity generated in such regions and that magma movement may be at the source of it all.

5. Summary

We have developed a method for investigating dyke injection in a controlled pressure and temperature environment using PMMA as an analogue injection material of high viscosity with which to pressurize an inner bore of a specimen material in tension and thus form and propagate a dyke. By using an array of AE sensors mounted around the specimen, we have compared and contrasted the seismic waveforms generated during the fracture event and during fluid flow after the fracture was formed. We conclude that the movement of this viscous fluid has the potential to generate low-frequency harmonic tremor similar to that observed in field-scale volcanic processes. We measure an overpressure (of the PMMA compared to confining pressure) required to initially form a dyke of around 12 MPa in basalt when confined at 30 MPa. These results are similar to previous studies, in which a lower pressure is then needed to continue dyke propagation. In both cases, a significant AE, analogous to field seismicity, is measured. We further conclude that the generation and stalling of magmatic dykes in shallow caldera systems is a likely source for much of the seismicity of such regions, as well as explaining some of the characteristic inflation and deflation.

Acknowledgments

This research was funded by the Swiss National Science Foundation (project 200021-137867). The authors would like to thank Robert Hofmann and Emily Butcher for their technical support and Marie Violay and Stephan Gehne for their fruitful discussions that have greatly improved this paper. D.B.D. and K.U.H. acknowledge the support of the ERC Advanced researcher grant EVOKES (247076). This paper includes supporting information including XCT scans and the raw data, which can be found in this journal's online resources.

References

- Bakker, R. R., M. E. S. Violay, P. M. Benson, and S. C. Vinciguerra (2015), Ductile flow in sub-volcanic carbonate basement as the main control for edifice stability: New experimental insights, *Earth Planet. Sci. Lett.*, *430*, 533–541, doi:10.1016/j.epsl.2015.08.017.
- Battaglia, M., C. Troise, F. Obrizzo, F. Pingue, and G. De Natale (2006), Evidence for fluid migration as the source of deformation at Campi Flegrei caldera (Italy), *Geophys. Res. Lett.*, *33*, L01307, doi:10.1029/2005GL024904.
- Benson, P. M., S. Vinciguerra, P. G. Meredith, and R. P. Young (2008), Laboratory simulation of volcano seismicity, *Science*, *322*(5899), 249–252, doi:10.1126/science.1161927.
- Benson, P. M., S. Vinciguerra, P. G. Meredith, and R. P. Young (2010), Spatio-temporal evolution of volcano seismicity: A laboratory study, *Earth Planet. Sci. Lett.*, *297*(1–2), 315–323, doi:10.1016/j.epsl.2010.06.033.
- Benson, P. M., M. J. Heap, Y. Lavallée, A. Flaws, K. U. Hess, A. P. S. Selvadurai, D. B. Dingwell, and B. Schillinger (2012), Laboratory simulations of tensile fracture development in a volcanic conduit via cyclic magma pressurisation, *Earth Planet. Sci. Lett.*, *349–350*, 231–239, doi:10.1016/j.epsl.2012.07.003.
- Brenner, S. L., and A. Gudmundsson (2004), Arrest and aperture variation of hydrofractures in layered reservoirs, *Geol. Soc. Lond. Spec. Publ.*, *231*, 117–128, doi:10.1144/GSL.SP.2004.231.01.08.
- Browning, J., and A. Gudmundsson (2015), Surface displacements resulting from magma-chamber roof subsidence, with application to the 2014–2015 Bardarbunga-Holuhraun volcanotectonic episode in Iceland, *J. Volcanol. Geotherm. Res.*, doi:10.1016/j.jvolgeores.2015.10.015.
- Burlini, L., S. Vinciguerra, G. Di Toro, G. De Natale, P. Meredith, and J. P. Burg (2007), Seismicity preceding volcanic eruptions: New experimental insights, *Geology*, *35*(2), 183–186, doi:10.1130/G23195A.1.
- Cartwright-Taylor, A., F. Vallianatos, and P. Sammonds (2014), Superstatistical view of stress-induced electric current fluctuations in rocks, *Phys. A Stat. Mech. Appl.*, *414*, 368–377, doi:10.1016/j.physa.2014.07.064.
- Chouet, B. (2003), Volcano seismology, *Pure Appl. Geophys.*, *4*, 739–788, doi:10.1016/B978-044452748-6.00073-0.
- Chouet, B. A. (1996), New methods and future trends in seismological volcano monitoring, in *Monitoring and Mitigation of Volcano Hazards SE—2*, pp. 23–97, Springer, Berlin, Heidelberg.
- D'Auria, L., et al. (2015), Magma injection beneath the urban area of Naples: A new mechanism for the 2012–2013 volcanic unrest at Campi Flegrei caldera, *Sci. Rep.*, *5*(April), 13,100, doi:10.1038/srep13100.
- De Natale, G., S. M. Petrazzuoli, and F. Pingue (1997), The effect of collapse structures on ground deformations in calderas, *Geophys. Res. Lett.*, *24*(13), 1555–1558, doi:10.1029/97GL01600.
- Fortin, J., S. Stanchits, S. Vinciguerra, and Y. Guéguen (2011), Influence of thermal and mechanical cracks on permeability and elastic wave velocities in a basalt from Mt. Etna volcano subjected to elevated pressure, *Tectonophysics*, *503*(1–2), 60–74, doi:10.1016/j.tecto.2010.09.028.
- Gudmundsson, A. (2002), Emplacement and arrest of sheets and dykes in central volcanoes, *J. Volcanol. Geotherm. Res.*, *116*(3–4), 279–298, doi:10.1016/S0377-0273(02)00226-3.
- Gudmundsson, A. (2003), Surface stresses associated with arrested dykes in rift zones, *Bull. Volcanol.*, *65*(8), 606–619, doi:10.1007/s00445-003-0289-7.

- Gudmundsson, A. (2011), Deflection of dykes into sills at discontinuities and magma-chamber formation, *Tectonophysics*, 500(1–4), 50–64, doi:10.1016/j.tecto.2009.10.015.
- Gudmundsson, A., and S. L. Brenner (2004), Local stresses, dyke arrest and surface deformation in volcanic edifices and rift zones, *Ann. Geophys.*, 47(4), 1433–1454.
- Gudmundsson, A., N. Lecoeur, N. Mohajeri, and T. Thordarson (2014), Dike emplacement at Bardarbunga, Iceland, induces unusual stress changes, caldera deformation, and earthquakes, *Bull. Volcanol.*, 76, 869, doi:10.1007/s00445-014-0869-8.
- Heap, M. J., S. Vinciguerra, and P. G. Meredith (2009), The evolution of elastic moduli with increasing crack damage during cyclic stressing of a basalt from Mt. Etna volcano, *Tectonophysics*, 471(1–2), 153–160, doi:10.1016/j.tecto.2008.10.004.
- Hieber, C. a., and H. H. Chiang (1992), Shear-rate-dependence modeling of polymer melt viscosity, *Polym. Eng. Sci.*, 32(14), 931–938, doi:10.1002/pen.760321404.
- Hoskins, E. R. (1969), The failure of thick-walled hollow cylinders of isotropic rock, *Int. J. Rock Mech. Min. Sci. Geomech. Abstr.*, 6, 99–125, doi:10.1016/0148-9062(69)90030-8.
- Kendrick, J. E., Y. Lavallée, A. Ferk, D. Perugini, R. Leonhardt, and D. B. Dingwell (2012), Extreme frictional processes in the volcanic conduit of Mount St. Helens (USA) during the 2004–2008 eruption, *J. Struct. Geol.*, 38, 61–76, doi:10.1016/j.jsg.2011.10.003.
- Kilburn, C. (2012), Precursory deformation and fracture before brittle rock failure and potential application to volcanic unrest, *J. Geophys. Res.*, 117, B02211, doi:10.1029/2011JB008703.
- Lavallée, Y., P. G. Meredith, D. B. Dingwell, K.-U. Hess, J. Wassermann, B. Cordonnier, A. Gerik, and J. H. Kruhl (2008), Seismogenic lavas and explosive eruption forecasting, *Nature*, 453(7194), 507–510, doi:10.1038/nature06980.
- McNutt, S. R. (1996), Seismic monitoring and eruption forecasting of volcanoes: A review of the state of the art and case histories, *Monit. Mitig. Volcano Hazards*, 99–146.
- Mori, J., R. A. White, D. H. Harlow, P. Okubo, J. A. Power, R. P. Hoblitt, E. P. Laguerta, A. Lanuza, and B. C. Bautista (1996), Volcanic earthquakes following the 1991 climactic eruption of Mount Pinatubo: Strong seismicity during a waning eruption, in *Fire and Mud: Eruptions and Lahars of Mount Pinatubo, Philippines*, pp. 339–350. [Available at <http://pubs.usgs.gov/pinatubo/mori1/>]
- Rivalta, E., B. Taisne, A. P. Bungler, and R. F. Katz (2015), A review of mechanical models of dike propagation: Schools of thought, results and future directions, *Tectonophysics*, 638, 1–42, doi:10.1016/j.tecto.2014.10.003.
- Santarelli, F. J., and E. T. Brown (1989), Failure of three sedimentary rocks in triaxial and hollow cylinder compression tests, *Int. J. Rock Mech. Min. Sci.*, 26(5), 401–413, doi:10.1016/0148-9062(89)90936-4.
- Sigmundsson, F., et al. (2015), Segmented lateral dyke growth in a rifting event at Bárðarbunga volcanic system, Iceland, *Nature*, 517(7533), 191–5, doi:10.1038/nature14111.
- Taisne, B., and S. Tait (2011), Effect of solidification on a propagating dike, *J. Geophys. Res.*, 116, B01206, doi:10.1029/2009JB007058.
- Vinciguerra, S., P. G. Meredith, and J. Hazzard (2004), Experimental and modeling study of fluid pressure-driven fractures in Darley Dale sandstone, *Geophys. Res. Lett.*, 31, L09609, doi:10.1029/2004GL019638.
- Vinciguerra, S., C. Trovato, P. G. Meredith, and P. M. Benson (2005), Relating seismic velocities, thermal cracking and permeability in Mt. Etna and Iceland basalts, *Int. J. Rock Mech. Min. Sci.*, 42(7–8 SPEC. ISS), 900–910, doi:10.1016/j.ijrmmms.2005.05.022.